Dalton Transactions

ROYAL SOCIETY OF CHEMISTRY

PAPER

View Article Online
View Journal | View Issue

Check for updates

Cite this: *Dalton Trans.*, 2025, **54**, 13918

Ansa-effects in alkaline earth metal octaphenylmetallocenophanes and a derived *ansa*-ferrocene

Angus C. G. Shephard,[a] Amal Bouammali,[b] Aymeric Delon,[a,c] Zhifang Guo,[a] Sylviane Chevreux,[c,d] Claude Niebel,[b] Olivier Dautel,[b] Thomas Simler,[e] Glen B. Deacon,[f] Peter C. Junk *[a] and Florian Jaroschik *[b]

Received 6th August 2025,
Accepted 26th August 2025

DOI: 10.1039/d5dt01881a

rsc.li/dalton

The synthesis and structural characterisation of a series of alkaline earth *ansa*-octaphenylmetallocenes (Mg, Ca, Sr, Ba) bearing an ethylene bridge are described. The complexes $[AE(C_5Ph_4CH_2)_2(thf)_n]$ (AE = Mg (**1**), Ca (**2**) n = 1; AE = Sr (**3**), Ba (**4**), n = 2) were obtained through reductive dimerisation of 1,2,3,4-tetraphenylfulvene, facilitated by zero-valent metals and fully characterised by NMR spectroscopy. Single-crystal XRD studies reveal distinct binding differences of the Cp ligands to Mg in complex **1** compared to the heavier analogues (η^3 *vs.* η^5). Complex **3** is the first structurally characterised *ansa*-metallocene complex of Sr. An *ansa*-effect was observed for the Ba complex **4** which showed good stability at room temperature in contrast to the previously described non-bridged analogue. Efficient transmetallation from the Ca *ansa* complex **2** to $FeCl_2$ provided the new *ansa*-ferrocene complex $[Fe(C_5Ph_4CH_2)_2]$ (**5**). Structural, spectroscopic and electrochemical properties of this bent ferrocenophane complex were compared to those of the known unbridged octaphenylferrocene.

Introduction

Connecting two cyclopentadienyl ligands *via* a carbon- or heteroatom-based bridge of variable chain length can significantly alter the coordination chemistry around a metal centre.[1–3] Furthermore, substantial changes can be induced in the stability and/or the reactivity of such organometallic complexes compared to their non-bridged analogues.[4–7] Even though iron-based *ansa*-metallocenes (also called ferrocenophanes) have been known since the 1960s,[8] a breakthrough was achieved by the pioneering works of Brintzinger and co-workers from the 1980s with chiral group 4 metal complexes.[9,10] This has led to many significantly improved polymerisation processes, a field that is currently still under investigation.[11–15] This concept of bridging ligands was rapidly extended to other metals but also to other aromatic carbocycles, such as indenyls, fluorenyls and many other π-systems.[16–26]

In the early 1990s, Edelmann and coworkers reported on the synthesis and characterisation of the first Ca and Sr *ansa* complexes *via* reductive dimerisation of 6,6-dimethylfulvene[27–29] induced by the corresponding alkaline earth (AE) metal.[30] Only the Ca-complex **A** could be structurally characterised after coordination with diazabutadiene (Fig. 1a). Interestingly, Ba metal was reported not to react under these conditions. Subsequently, several other examples of Mg and Ca *ansa* complexes were synthesised, notably by Shapiro and coworkers,[31,32] whereas Sr and Ba complexes still remain scarce.[33,34] Comprehensive reviews by Schäfer and Mukherjee nicely summarise the advances in this domain.[35,36] The main application of these complexes lies in the transmetallation of the *ansa*-ligand system to other main group or transition metals, providing efficient catalytic systems or complexes with biological activity.[37,38] Recent studies showed the applicability of *ansa*-magnesocene complexes in the catalytic cross-dehydrocoupling of amines and silanes or boranes.[39,40] Theoretical studies have been reported on the formation of the AE *ansa* complexes *via* reductive dimerisation,[41] as well as the structural influences of bridge length and coordinated solvent molecules on various AE complexes.[42]

PolyarylCp chemistry of AE metals is far less developed than the corresponding polyalkylCp chemistry.[43] In Hanusa's early work, the Ba-tetraphenylCp sandwich complex [Ba

[a]College of Science and Engineering, James Cook University, Townsville 4811, Australia. E-mail: peter.junk@jcu.edu.au
[b]ICGM, Univ. Montpellier, CNRS, ENSCM, 34090 Montpellier, France. E-mail: florian.jaroschik@enscm.fr
[c]Université de Reims Champagne Ardenne, CNRS, ICMR UMR 7312, 51097 Reims, France
[d]Institut de Recherche de Chimie Paris, UMR CNRS 8247 Chimie ParisTech, PSL University, 75005 Paris, France
[e]LCM, CNRS, École Polytechnique, Institut Polytechnique de Paris, 91120 Palaiseau, France
[f]School of Chemistry Monash University Clayton, Vic, 3800, Australia

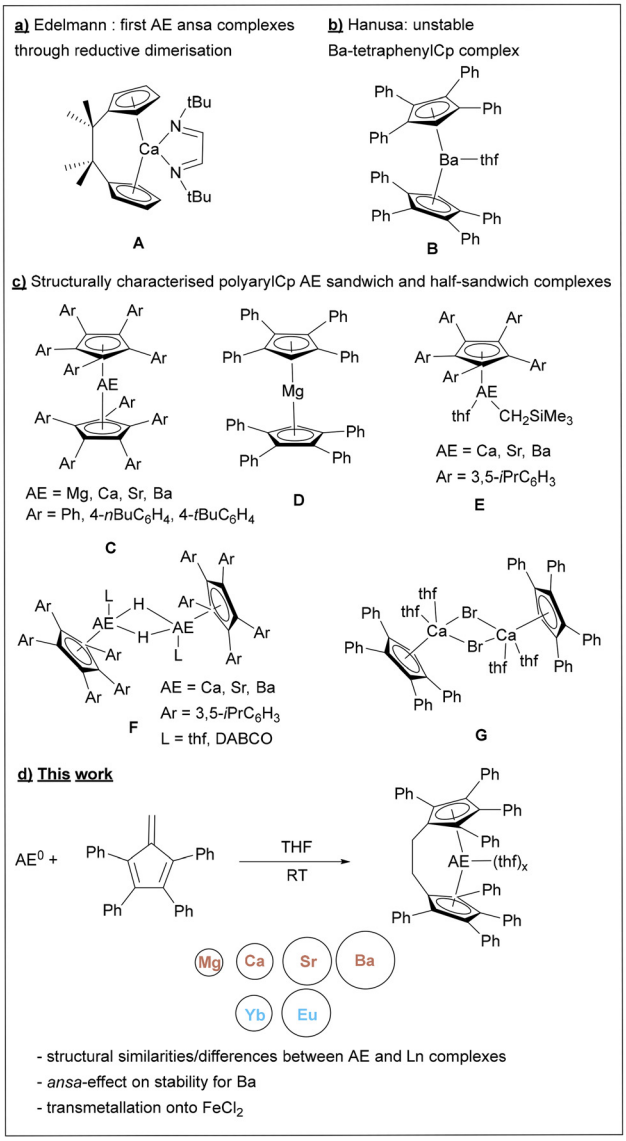

Fig. 1 Literature overview on first AE-*ansa* (a) and isolated AE-polyarylCp complexes (b) and (c) and this work (d).

$(C_5Ph_4H)_2(thf)]$ **B**, obtained *via* a protolysis reaction from [Ba$(N(SiMe_3)_2)_2$] and $C_5PH_4H_2$, was reported to decompose at room temperature, hence limiting structural characterisations to NMR studies (Fig. 1b).[44] The corresponding decaphenylbarocene [Ba$(C_5Ph_5)_2$], did not form at all under these conditions. Several contributions from the Harder, Schulz, Cheng, and our groups have shown new synthetic possibilities and some applications in this field.[45–49] Protolysis reactions with different benzylic or alkyl group 2 precursors provided access to decaarylmetallocenes [M$(C_5Ar_5)_2$] (Ar = 4-*n*BuC_6H_4) **C** and octaphenylmagnesocene [Mg$(C_5Ph_4H)_2$] **D** (Fig. 1c).[45,46] With very bulky pentaarylCp ligands, the mixed mono-Cp AE alkyl complexes [(C_5Ar_5)AE(CH_2SiMe_3)(thf)] **E** (Ar = 3,5-iPrC_6H_3) were obtained, which could be further transformed to the dimeric hydride complexes **F**. The latter showed good activity in the hydrogenation of alkenes.[47] Approaches involving oxidation of zerovalent AE metals using either organomercury reagents for redox transmetallation/protolysis (RTP) reactions[46,48] or cyclopentadienyl radicals[49] yielded mostly the sandwich complexes **C** for Ar = Ph or 4-*t*BuC_6H_4. When PhHgBr was employed as an oxidant in the RTP process, the Ca half-sandwich complex [(C_5Ph_4H)CaBr$(thf)_2]_2$ **G** could be isolated in good yields (Fig. 1c).[46]

In our ongoing work on the synthesis of polarylCp lanthanoid complexes, we have recently reported an *ansa*-effect in the luminescence properties of divalent octaphenyleuropocenes.[50] A significantly red-shifted emission coupled with an increased emission lifetime was observed for the *ansa* complex [Eu$(C_5Ph_4CH_2)_2(thf)_2$] compared to its non-bridged analogue [Eu$(C_5Ph_4H)_2$(dme)]. The analogous divalent *ansa* complexes of Yb and Sm were also synthesised and structurally characterised.

Building on these results, the aim of the current work was to extend the previously described reductive dimerisation of 1,2,3,4-tetraphenylfulvene from lanthanoid to alkaline earth metals, in order to (i) investigate a potential *ansa*-effect to stabilise the Ba complex; (ii) verify the structural analogies often described for Ca and Yb as well as for Sr and Eu/Sm; (iii) examine the structural differences that the smaller Mg and the much larger Ba could provide (Fig. 1d). Additionally, the transmetallation reaction of the Ca-*ansa* complex with $FeCl_2$ was probed to access the first bridged transition-metal octaphenylmetallocene.

Results and discussion

Synthesis of *ansa*-AE complexes *via* reductive dimerisation

Historically, the synthesis of group 2 and lanthanoid *ansa* complexes by reductive dimerisation has utilised a range of reaction conditions and stoichiometric ratios of metal to fulvene.[27–32] Previously, we described the synthesis of divalent *ansa*-octaphenyllanthanocene complexes of samarium, europium and ytterbium by employing a 2 : 1 ratio of metal : fulvene in THF, with a crystal of iodine for metal activation, and stirring the resulting mixture for 72 hours.[50] Following suit, these reaction conditions were initially employed for the attempted synthesis of *ansa*-octaphenylmagnesocene [Mg$(C_5Ph_4CH_2)_2(thf)$] (**1**) (Scheme 1). However, it turned out that in this case a 4 : 1 ratio of Mg : fulvene provided the best results.

Compared to the analogous synthesis involving Ln metals, considerably more insoluble material was observed after 72 hours when magnesium turnings were used. The supernatant solution was found to only contain small amounts of unreacted fulvene, whilst the pale yellow-green precipitate could be solubilised in hot benzene or toluene and was identified as the Mg-*ansa* complex [Mg$(C_5Ph_4CH_2)_2(thf)$] (**1**). Once dissolved, the material remained soluble, even upon cooling. Crystals suitable for X-ray diffraction were grown from a layering of *n*-pentane over a toluene solution of **1**, affording the *ansa* metallocene complex **1·Toluene** as yellow needles (Fig. 2).

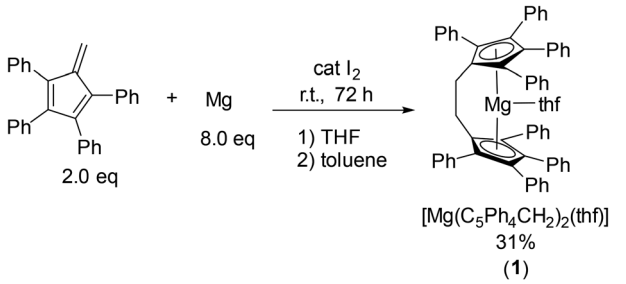

Scheme 1 Synthesis of $[Mg(C_5Ph_4CH_2)_2(thf)]$ (**1**) by reductive dimerisation of 1,2,3,4-tetraphenylfulvene with activated Mg metal.

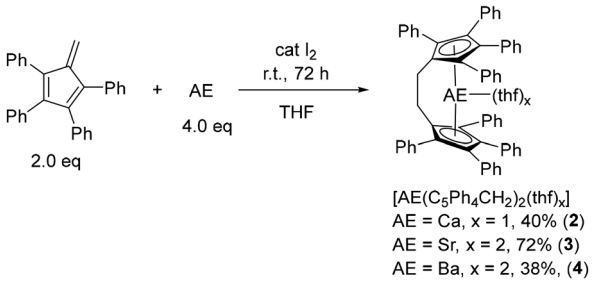

Scheme 2 Synthesis of calcium (**2**), strontium (**3**) and barium (**4**) *ansa* metallocene complexes by reductive dimerisation of 1,2,3,4-tetraphenylfulvene.

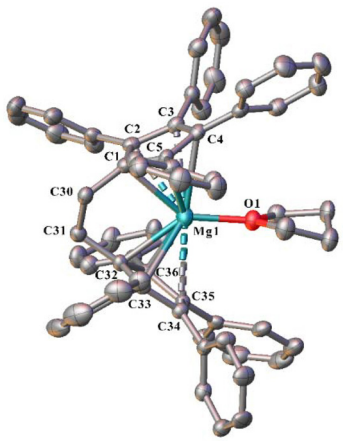

Fig. 2 ORTEP diagram of complex **1**·Toluene showing atom-numbering scheme for relevant atoms. Thermal ellipsoids are drawn at the 50% probability level. Hydrogen atoms and lattice solvent are omitted for clarity. Selected bond lengths in (Å): Mg(1)–C(1) 2.412(3), Mg(1)–C(2) 2.677(3), Mg(1)–C(3) 2.750(3), Mg(1)–C(4) 2.580(3), Mg(1)–C(5) 2.332(3), Mg(1)–C(32) 2.331(4), Mg(1)–C(33) 2.586(3), Mg(1)–C(34) 2.790(3), Mg (1)–C(35) 2.669(3), Mg(1)–C(36) 2.344(3) Mg(1)–O(1) 2.008(3).

Whereas already described *ansa* metallocenes of group 2 metals are primarily based on magnesium and calcium, their strontium and barium counterparts are far less documented.[35,36] Alongside this, there is no report on a structurally characterised strontium *ansa* metallocene complex. Accordingly, the established methodology was extended to calcium, strontium, and barium in order to access their corresponding *ansa* metallocene complexes. Similar reaction conditions, with metal filings in a 2 : 1 ratio of metal : fulvene, afforded complexes of the general form $[AE(C_5Ph_4CH_2)_2(thf)_n]$ (AE = Ca (**2**), n = 1, Sr (**3**), n = 2, and Ba (**4**), n = 2) in moderate to good yields (Scheme 2). In all cases, considerably less insoluble material was observed when compared to the reaction with magnesium, and as such, the supernatant solutions were separated by filtration and either evaporated to dryness and the residue crystallised from THF (in the case of **2** and **3**), or, in the case of **4**, concentrated directly to induce crystallisation at room temperature. Satisfactory elemental analyses or MALDI-TOF mass spectra were obtained for all complexes.

NMR spectroscopy

Complexes **1–4** were analysed by ^{1}H and ^{13}C NMR spectroscopy in C_6D_6, with the characteristic CH_2–CH_2 bridge shifts being summarised in Table 1. Most notably, the spectra showed striking similarity to those of the previously described diamagnetic ytterbium(II) analogue $[Yb(C_5Ph_4CH_2)_2(thf)]$ in C_6D_6, with resonance for the CH_2–CH_2 tether appearing at 3.44 ppm and 27.8 ppm for the ^{1}H and $^{13}C\{^1H\}$ NMR spectra respectively.[50] In all cases, the CH_2–CH_2 bridge appeared as a distinct singlet in the range of 3.2 to 3.5 ppm in the ^{1}H NMR spectra, and between 27.2 and 27.9 in the $^{13}C\{^1H\}$ NMR spectra. For the Cp carbons, in the $^{13}C\{^1H\}$ NMR spectra, signals were observed between 124 and 125 ppm for the heavier complexes **2–4**. In the case of the Mg complex **1**, two particularly shifted signals were observed at 117 and 121 ppm, in agreement with a variation in coordination mode, as observed in the solid state (see below). It should be noted that even though the complexes were isolated as thf-solvates, no difference between coordinated and free THF was observed in the ^{1}H NMR spectrum, probably due to rapid exchange processes at the metal center.[46]

X-ray diffraction studies of *ansa*-AE complexes

Single crystal X-ray diffraction studies were undertaken on complexes **1–4**, however for complex **2** only connectivity could be established. All complexes consist of the same general arrangement, of the metal cation ligated by two bent cyclopentadienyl moieties which are bridged by a CH_2–CH_2 tether, and one (Mg (**1**) and Ca (**2**)) or two (Sr (**3**) and Ba (**4**)) THF molecules, analogous to the Yb, and Sm and Eu complexes respect-

Table 1 Summary of ^{1}H and ^{13}C NMR chemical shifts (in C_6D_6) of the CH_2–CH_2 bridge in complexes **1–4**

Complex	^{1}H NMR chemical shift (ppm)	$^{13}C\{^1H\}$ NMR chemical shift (ppm)
Yb[50]	3.44	27.8
1 (Mg)	3.22	27.9
2 (Ca)	3.43	27.5
3 (Sr)	3.49	27.6
4 (Ba)	3.43	27.2

Table 2 Comparison of the bond lengths (Å), angles (°), slippage (°), and slip parameter (Å) of complexes **1**·Toluene, **3**·3 THF and **4**·2 THF with the analogous divalent lanthanoid *ansa* complexes (in order of increasing ionic radius)[50]

Parameter	**1**·Toluene (Mg)	[Yb $(C_5Ph_4CH_2)_2(thf)$]	[Eu $(C_5Ph_4CH_2)_2(thf)_2$]	**3**·3 THF (Sr)	[Sm $(C_5Ph_4CH_2)_2(thf)_2$]	**4**·2 THF (Ba)
Ionic radius	0.72–0–89[a]	1.08	1.25	1.26	1.27	1.42
Coordination number (see note †)	7	7	8	8	8	8
M–Cn(1)	2.244(2)	2.411(1)	2.616(2)	2.646(2)	2.625(2)	2.852(1)
M–Cn(2)	2.250(2)	2.415(1)	2.625(2)	2.643(2)	2.627(3)	2.813(1)
M–O(1)	2.006(2)	2.389(2)	2.605(3)	2.607(3)	2.646(4)	2.809(3)
M–O(2)	—	—	2.628(3)	2.584(3)	2.613(4)	2.828(3)
C(1)–C(30)–C(31)–C(32) (dihedral angle)	57.3(3)	59.5(3)	60.1(4)	59.8(4)	59.7(5)	68.5(3)
A (intersection angle of Cp planes)	43.3(2)	55.4(1)	64.2(1)	64.8(6)	64.2(1)	68.4(1)
Cn(1)–M–Cn(2) (γ)	136.8(1)	124.6(1)	115.8(1)	115.2(1)	115.2(1)	111.7(1)
Cn(1)–Cn(2) (β)	120.8(2)	120.5(1)	111.7(2)	111.5(2)	112.0(2)	106.5(1)
Slippage (γ–β)	16.0	4.1	4.1	3.7	3.8	5.2
Slip parameter ($\Delta_{(M-C)}$)[b]	0.27–0.31	0.07–0.16	0.05–0.06	0.04–0.06	0.04–0.06	0.19–0.20

[a] No data for Mg^{2+} with a coordination number of 7 is available, thus the selected radius represents a value between CN6 and CN8. [b] See eqn (S1) in SI for definition.

ively.† In contrast to previously described AE octa and pentaarylmetallocenes, none of the new complexes **1–4** exhibit a unidirectional propeller-like arrangement of the phenyl rings.[45–49] This may be related to the steric hindrance brought about by the tether. Nevertheless, intra- and inter-ligand non-classical C–H–C π-bonds between neighbouring phenyl groups are present in all complexes. Selected bond lengths and angles for **1**, **3**, and **4** have been summarised in Table 2, alongside those of the analogous divalent lanthanoid complexes.[50] Overall, there is no major variance in the torsion angle C(1)–C(30)–C(31)–C(32) of **1** and **3** with their Ln counterparts, however, the large Ba^{2+} cation in **4** causes a deviation from this trend, with an increased dihedral angle.

Complex **1** crystallises in the trigonal space group $R\bar{3}$ (Fig. 2) with one molecule of toluene in the lattice, alongside fractions of disordered molecules of pentane. The bent arrangement in **1** with a Cn–Mg–Cn (Cn = ring centroid) angle of 136.8(1)° is significantly different from the previously described octaphenyl [$Mg(C_5Ph_4H)_2$] and decaaryl [$Mg(C_5(4\text{-}tBu\text{-}C_6H_4)_5)_2$] magnesocenes.[46,49] Both reported sandwich complexes are perfectly linear, with a Cn–Mg–Cn bond angle of 180°, and adopt an η^5 coordination mode. Note that the octaphenyl complex exhibits minor skewing owing to the asymmetry of the ligand with Mg–C bond distances ranging from 2.291(2) to 2.422(2) Å. In the latter complex the Cn–Mg bond distances are 2.016(12) and 2.063(6) Å, which are considerably shorter than those observed in complex **1** (2.245(2) and 2.244(2) Å). As observed by Burger and co-workers,[51] introduction of a CH_2–CH_2 bridge results in the bent orientation of the Cp planes about the Mg centre, and the resulting coordination gap is filled by coordinating solvent, affecting the hapticity of the Cp moieties. In **1**, the Mg–C bond distances for the two Cp moieties are non-uniform, going from 2.331(4) to 2.790(3) Å (see Fig. 2), indicative of a deviation from the classical η^5 coordination. In order to evaluate this ring slippage, two different parameters have been introduced in the literature. For *ansa*-complexes, the ring slippage is often considered, which is defined as the difference of the angles γ–β, where γ represents the angle between the vectors from the metal to the ring centroids and β the angle between the vectors normal to the ring centroids (see Table 2 and Fig. 4).[1] For **1**, this angle has a high value of 16°, whereas typical η^5 complexes, such as the *ansa*-lanthanoid analogues (Sm, Eu) display angles around 4° (Table 2). Alternatively, in Mg and transition-metal indenyl complex, a slip parameter Δ_{M-C} was defined according to eqn (S1) (see SI).[52–54] For the η^3-bound $Mg(indenyl)_2$ complex, a Δ_{M-C} value of 0.27 Å was calculated,[55] whereas for a recent di-Mg-pentalenide complex $[MgBu(thf)_2]_2[Ph_4Pn]$, a Δ_{M-C} value of 0.23 Å was obtained.[56] Applying eqn (S1) to complex **1**, a Δ_{M-C} value of 0.27–0.31 Å was calculated (see Table S2), pointing towards a hapticity change from η^5 to η^3-like for both Cp ligands. This corroborates with the high value for the slippage angle of **1**. This η^3-like coordination of the Cp moiety is also in agreement with the observations in the $^{13}C\{^1H\}$ NMR spectrum described above. Compared to a representative *ansa* complex, $[Mg(Cp^{tBu}C(CH_3)_2)_2(thf)]$,[57] a similar shift in hapticity is observed for one of the Cp ligands (Δ_{M-C} = 0.13 Å, see Table S3), with Mg–C bond distances ranging from 2.342 to 2.525 Å, though a smaller range than for **1**. Furthermore, the dihedral angle of the $(C(CH_3)_2)_2$ bridge (22.8(2)°) is much less pronounced than that of complex **1** (57.7(3)°), likely as a result of the bulky methyl substituents in the former restricting its flexibility. Along this line, it should be noted, that the previously reported Yb *ansa*-complex revealed two Δ_{M-C} values of 0.07 and 0.16 Å, clearly showing deviation from η^5 coordination for one of the Cp ligands (Table 2). However, the slip-

† The ionic model for determining coordination numbers is employed with each Cp ligand counting for **3** and each THF ligand for **1**.

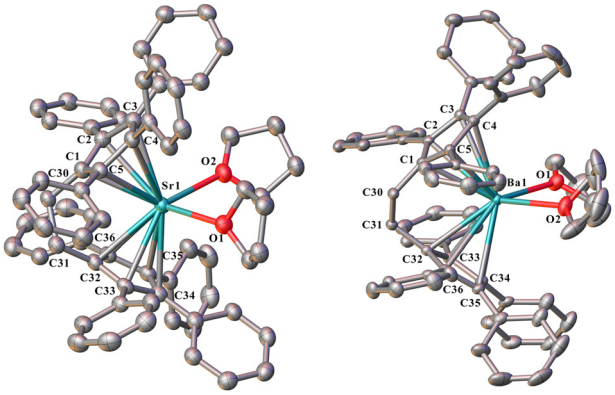

Fig. 3 ORTEP diagram of complex **3**·3 THF (left) and **4**·2 THF (right) showing atom-numbering scheme for relevant atoms. Thermal ellipsoids are drawn at the 50% probability level. Hydrogen atoms and lattice solvent are omitted for clarity. Selected bond lengths of **3**·3 THF (Å): Sr(1)–Cn(1) 2.645(2), Sr(1)–Cn(2) 2.643(2), Sr(1)–O(1) 2.607(3), Sr(1)–O(2) 2.584(3); and **4**·2 THF (Å): Ba(1)–Cn(1) 2.825(1), Ba(1)–Cn(2) 2.813(1), Ba(1)–O(1) 2.828(3), Ba(1)–O(2) 2.809(3).

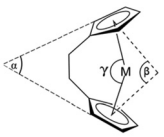

Fig. 4 Visual representation of geometric parameters, α, γ and β, in a generic C_2 *ansa* complex.

page angle of 4.1° did not reflect this Cp ligand shift, as this value was close to the η^5 bound Eu and Sm complexes (3.8–4.1°, Δ_{M-C} = 0.04–0.06 Å) (Table 2). Consequently, Δ_{M-C} can provide more information on ring slippage, as will be seen further below.

Complex **2** crystallises with three molecules of THF in the lattice in the *C*2/*c* space group, and is isomorphic to the previously reported [Yb($C_5Ph_4CH_2$)$_2$(thf)] complex (unit cell of **2**: *a* = 43.60, *b* = 12.39, *c* = 20.94, *β* = 93.4°; unit cell of [Yb($C_5Ph_4CH_2$)$_2$(thf)]: *a* = 43.66, *b* = 12.38, *c* = 20.94, *β* = 93.6°).[50] Repeated attempts to obtain satisfactory data for **2** were undertaken, however, only connectivity of the complex could be established (see SI for ORTEP diagram). Whilst several Ca *ansa* metallocene complexes with a C–C bridge are known, they typically exhibit a coordination number of 8 (see [Ca(Cp(CPh)$_2$)$_2$(thf)$_2$],[58] and [Ca($C_5Me_4CH_2$)$_2$(thf)$_2$]).[38] Complex **2** is rather unique in that the steric influence of the phenyl groups around the Cp moieties restricts the coordination number to 7.

Complexes **3** and **4** both crystallise in the monoclinic space group $P2_1$ (Fig. 3), with three and two THF molecules in their respective lattices. Despite there being several examples of strontium *ansa* metallocene complexes described in the literature, complex **3** is the first to have been structurally characterised by single crystal X-ray diffraction studies. Owing to this, there is limited comparison to be made, as the corresponding octaphenyl strontocene has not been structurally characterised. When compared to the somewhat analogous pentaaryl strontocene complexes, the strontium to centroid bond distances of **3** (Sr(1)–Cn(1) = 2.646(2) and Sr(1)–Cn(2) = 2.643(2) Å) are considerably longer than those of [Sr(C_5(4-*n*Bu-C_6H_4)$_5$)$_2$] (Sr(1)–Cn = 2.513(1)),[45] [Sr(C_5(4-*t*Bu-C_6H_4)$_5$)$_2$] (Sr(1)–Cn(1) = 2.492 Å and Sr(1)–Cn(2) = 2.495 Å),[49] after correcting for differences in ionic radii (Sr^{2+} 1.18 Å, CN = 6; Sr^{2+} 1.26 Å, CN = 8).[59] As the ionic radii of Sr^{2+}, Eu^{2+}, and Sm^{2+} cations are very similar (1.26 *vs.* 1.25 and 1.27 Å respectively for eight-coordinate cations),[59] analogous complexes of Sr, Eu and Sm metals show similar structural properties, and as such, a better comparison can be drawn by comparing **3** with the previously reported [Ln($C_5Ph_4CH_2$)$_2$(thf)$_2$] complexes of Eu and Sm.[50] The three complexes exhibit comparable metal to centroid distances (Sr(1)–Cn(1) = 2.646(2) and Sr(1)–Cn(2) = 2.643(2) Å *versus* Eu(1)–Cn(1) = 2.616(2) and Eu(1)–Cn(2) = 2.625(2) Å and Sm(1)–Cn(1) = 2.625(2) and Sm(1)–Cn(2) 2.627(3) Å). The Cn(1)–Sr(1)–Cn(2) angle of 115.2(1)° is also very close to that of the Cn(1)–Eu(1)–Cn(2) angle of 115.8(1)°, and 115.8(1)° for Cn(1)–Sm(1)–Cn(2). All three complexes exhibit low slippage angles from 3.7 to 4.1° and Δ_{M-C} values between 0.04 to 0.06 Å in agreement with η^5 Cp-ligand coordination.

In the case of complex **4**, the planes of the two cyclopentadienyl rings are at an angle of 111.7(1)° with respect to the barium centre (*i.e.* Cn(1)–Ba(1)–Cn(2)) which is considerably smaller than that of **3** owing to the much larger ionic radius of the eight-coordinate Ba^{2+} cation compared to that of the eight-coordinate Sr^{2+} cation (1.42 Å *vs.* 1.26 Å respectively).[59] Both octa- and deca-phenyl barocenes have been reported,[44,48] however, no X-ray crystal structures have been obtained for the more comparable octaphenyl barocene.[44] Complex **4** exhibits barium to centroid distances of 2.813(1) and 2.825(1) Å, considerably longer than those of decaphenyl barocene (2.670 Å), but this elongation is common among barocene species that do not display a parallel, planar Cp arrangement.[60,61] The large ionic radius of the Ba^{2+} cation, when compared to the smaller Sr^{2+} cation, leads to a larger slippage angle (3.7° *vs.* 5.2°), however the observed ring shift away from pure η^5-coordination mode in the Ba complex is even more pronounced when considering the Δ_{M-C} values, with 0.04 Å for **3** *vs.* 0.19–0.20 Å for **4** (Table S4 and S5).

Transmetallation reaction

Various transition metal octaphenylmetallocenes have been described in the literature, including Fe, Ru, Ti, however, to the best of our knowledge no related *ansa*-bridged example has been reported.[62–66] To examine the transmetallating properties of the new Ca-*ansa* complex **2**, which was selected based on Ca being the most abundant and least toxic metal in the group 2 series, and to study the influence of the bridge in transition-metal complexes, we have synthesised and fully characterised the *ansa*-octaphenylferrocene complex **5**. Indeed, iron *ansa* complexes have been studied for a long time for their coordination behaviour, their reactivity, especially for the production of metallapolymers, and their biomedicinal applications.[67–74] Reaction of equimolar amounts of **2** with

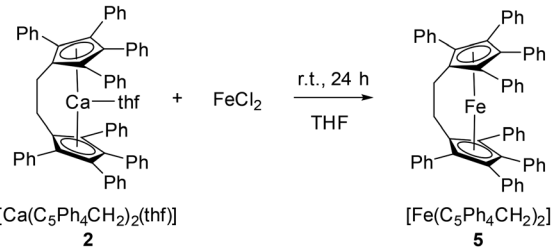

Scheme 3 Synthesis of *ansa* ferrocene complex **5** *via* transmetallation with **2** and $FeCl_2$.

$FeCl_2$ in THF at room temperature afforded, after filtration of the formed $CaCl_2$ and workup, the new *ansa*-ferrocene [Fe$(C_5Ph_4CH_2)_2$] **5** as a dark red powder in a very good (94%) yield (Scheme 3). HR ESI-MS confirmed the identity of the complex.

Crystals of complex **5** suitable for XRD analysis were obtained from a saturated THF/pentane solution at −20 °C. Complex **5** crystallises in the tetragonal space group $I4_1/a$, with two molecules of THF in the lattice. It is comprised of a 6-coordinate Fe^{2+} centre, ligated by the *ansa* ligand in a bent fashion, with no coordinated solvent (Fig. 5).†

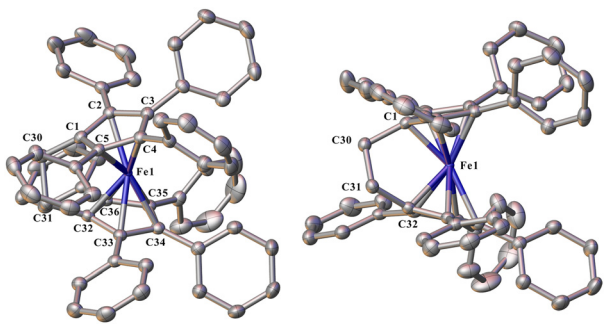

Fig. 5 ORTEP diagram of complex **5**·2 THF showing atom-numbering scheme for relevant atoms. Left: showing the η^5 coordination mode of Cp to Fe; right: showing the *ansa* bridge. Thermal ellipsoids are drawn at the 50% probability level. Hydrogen atoms and lattice solvent are omitted for clarity. Selected bond lengths (Å): C(1)–Fe(1) 2.000(2), C(2)–Fe(1) 2.074(2), C(3)–Fe(1) 2.107(2), C(4)–Fe(1) 2.096(2), C(5)–Fe(1) 2.098 (2), C(32)–Fe(1) 1.996(2), C(33)–Fe(1) 2.072(2), C(34)–Fe(1) 2.113(2), C(35)–Fe(1) 2.101(2), C(36)2.089(2) Fe(1)–Cn(1) 1.676(1), Fe(1)–Cn(2) 1.676(1).

Owing to the smaller size of the Fe^{2+} cation and the more covalent bonding character involving the d-orbitals, the structural parameters of complex **5** vary considerably from the above reported highly ionic AE *ansa* complexes. Most notably, the Cn(1)–Fe(1)–Cn(2) angle of 161.5(1)° represents the largest angle of the *ansa* series, a stark difference to the untethered tetraphenyl analogue, [Fe$(C_5Ph_4H)_2$], as well as the decaphenyl analogue, [Fe$(C_5Ph_5)_2$] which both exhibit a linear coordination mode with Cn–Fe–Cn angles of 180° (Table 3).[62,75] The bond distances from the Fe centre to the Cp carbons vary by approximately 0.1 Å across the complex **5** (1.996(2) to 2.113(2) Å, with an average of 2.075(2) Å). These are in line with the average Fe–C bond distances of the octa- and decaphenyl-ferrocene complexes previously reported (2.094(3) and 2.164(6) Å respectively), with **5** displaying slightly shorter Fe–C distances than its untethered counterpart. The slippage parameter of **5** was found to be 5.3°, a value comparable to that of the Ba^{2+} complex **4**. However, a huge difference in $\Delta_{(M-C)}$ was observed: for the *ansa*-ferrocene **5** a typical value for η^5-coordination mode was determined (0.04–0.05 Å), while the Ba *ansa*-complex showed a value of 0.19–0.20 Å, indicative of deviation from η^5-coordination. Once again, the $\Delta_{(M-C)}$ provides more information about the coordination situation than the slippage angle. In **5**, the dihedral angle of the C(1)–C(30)–C(31)–C(32) linkage is 47.4(2)°, significantly smaller than that described for **1–4**, owing to the short Fe–C bond lengths and comparatively small metal centre, yet considerably larger than that of unsubstituted [Fe$(C_5H_4CH_2)_2$], which has a dihedral angle of 35.1(9)°,[76] and much larger than the tetramethyl tethered [Fe$(C_5H_4(CH_3)_2)_2$] angle of 25.4°.[77] It should further be mentioned that numerous inter and intraligand non-classical C–H–C π-bonds between the phenyl rings, often observed in octa and decaphenylmetallocenes, are present and certainly also play a role in the geometry of complex **5**.

Compound **5** is stable in air in the solid state and in solution for several days. It shows similar characteristics in the IR spectrum and the ^1H and $^{13}C\{^1H\}$ NMR spectra (in THF-d_8) to the AE metal complexes, with the ethylene bridge at 3.24 ppm and 33.6 ppm, respectively. Comparative NMR studies between

Table 3 Comparison of the bond lengths (Å), angles (°), slippage (°) and and slip parameter (Å) of complex **5** with related iron complexes[62,75,76]

Parameter	5·2 THF (Fe)	[Fe$(C_5Ph_4H)_2$]	[Fe$(C_5Ph_5)_2$]	[Fe$(CpCH_2)_2$]
Ionic radius	0.61	0.61	0.61	0.61
Coordination number (see note †)	6	6	6	6
M–Cn(1)	1.676(1)	1.695(1)	1.723(1)	1.630(3)
M–Cn(2)	1.676(1)			1.628(3)
C(1)–C(30)–C(31)–C(32) (dihedral angle)	47.3(2)	—	—	35.1(9) and 41.9(2)[a]
α (intersection angle of Cp planes)	18.5(4)	—	—	15.8(2)
Cn(1)–M–Cn(2) (γ)	161.5(1)	180.0	180.0	164.2(2)
Cn(1)–Cn(2) (β)	156.2(1)	180.0	180.0	158.4(3)
Slippage (γ–β)	5.3	0.0	0.0	5.8
Slip parameter ($\Delta_{(M-C)}$)	0.044–0.055	—	—	0.059–0.065

[a] Significant disorder is observed along the *ansa* bridge, resulting in two distinct dihedral angles for this complex.

5 and the unsubstituted analogue, $[Fe(C_5Ph_4H)_2]$, revealed only differences in the $^{13}C\{^1H\}$ NMR shifts of the Cp carbons (82.7, 94.0, 95.0 ppm and 67.2, 86.1, 92.0 ppm respectively) which is to be expected when substituting the Cp proton of the C_5Ph_4H ligand with a CH_2CH_2 bridge.[62]

The UV/vis spectrum of **5** in dichloromethane shows strong absorptions at 286 nm and 301 nm, with a shoulder at 345 nm, as well as a weak broad absorption at 500 nm, similar to those of the non-bridged octaphenylferrocene (262 nm, 340 nm, 502 nm).[62] While it has been noted that non-linearity of ferrocenes can significantly affect the absorption spectra of these complexes leading to stronger absorptions at higher wavelengths,[77,78] the bending in **5** does not have a significant effect.

Cyclic voltammetry studies of **5**, conducted in dichloromethane solution using an Ag/Ag^+ reference electrode with 0.1 M TBAP (tetrabutylammonium perchlorate) as the supporting electrolyte (see SI), showed only a small influence of the introduction of the *ansa*-bridge on the $E^{1/2}$ value compared to the unbridged octaphenylferrocene (0.06 V *vs.* 0.10 V with respect to the Ag/Ag^+couple).[62] The value for **5** is therefore very close to the parent ferrocene $Fe(C_5H_5)_2$ (0.07 V). This further suggests that there is no major influence of the bent structure of the *ansa*-ferrocene on the electronic properties. Nevertheless, the reversibility of the redox-processes observed indicates the stability of the oxidized ferrocenophanium complex,[71] which will be further investigated in future studies.

Experimental

Materials and general procedures

All manipulations were performed under nitrogen, using standard Schlenk techniques. Solvents (THF and toluene) were distilled from sodium benzophenone before use, whilst hexane and pentane were purified by a solvent purification system. 1,2,3,4-tetraphenylfulvene was prepared by the literature method.[50] Infrared spectra (4000–400 cm^{-1}) for **1–4** were obtained as Nujol mulls between NaCl plates with a Nicolet-Nexus FT-IR spectrometer. The Infrared spectrum for **5** was collected using a PerkinElmer Spectrum 100 FT-IR spectrophotometer equipped with ATR or transmission modules. Absorption bands are reported in wavenumbers (cm^{-1}) and are designated as strong (s), medium (m), or weak (w). ^1H and $^{13}C\{^1H\}$ NMR spectra were recorded with a Bruker 400 MHz spectrometer. The chemical shifts were referenced to residual protio solvent peaks (^1H) or the deuterated solvent ($^{13}C\{^1H\}$). UV-Vis spectra were obtained using a JASCO V-770 spectrophotometer with a dual-beam configuration. Matrix-free LDI-MS experiments were performed on a MALDI micro MX mass spectrometer (Waters/Micromass Manchester UK) equipped with a N_2 laser (λ = 337 nm, 4 ns pulse duration up to 20 Hz repetition rate and max 320 μJ per pulse) in the positive-ion mode for data acquisition. HR ESI-MS data for **5** were obtained in the positive mode using a Synapt G2-S (UEB205-Waters) spectrometer. Cyclic Voltammetry experiments were performed with a potentiostat/galvanostat (Princeton Applied Research – AMETEK VersaSTAT4) driven by the VersaStudio software (V2.50.3), in a three-electrode cell containing 0.1 M tetrabutylammonium perchlorate (TBAP) in CH_2Cl_2, using Pt wires as working and counter electrodes and an Ag wire as a pseudo-reference electrode respectively. All potentials were recalibrated and reported using the Ferrocenium/Ferrocene couple as internal reference. All Cyclic Voltammograms (CVs) were recorded at a scan rate of 0.1 V s^{-1}. Crystal data and refinement details are given in Table S1. CCDC numbers 2464826 for **1**, 2464827–2464829 for **3–5** contain the supplementary crystallographic data for this paper.

Syntheses

$[Mg(C_5Ph_4CH_2)_2(thf)]$ (1). A Schlenk flask was charged with 1,2,3,4-tetraphenylfulvene (0.200 g, 0.524 mmol), magnesium metal strips (0.050 g, 2.1 mmol) and a crystal of iodine. Anhydrous THF (5 mL) was added, and the reaction mixture stirred for 72 hours. A pale green precipitate had formed, with a dark orange supernatant solution. The supernatant solution was removed by filtration, and the green solids dried under reduced pressure. The solids were then suspended in toluene (5 mL) and warmed gently to dissolve the material. The resulting solution was separated from unreacted magnesium strips by filtration, dried under reduced pressure, and washed with anhydrous hexane (5 mL) yielding **1** as a beige solid (0.065 g, 31%). Colourless needles suitable for X-ray diffraction studies of **1·Toluene** could be grown by layering a toluene solution of **1** with *n*-pentane. Anal. calc. for $C_{64}H_{52}OMg$ (861.40 g mol^{-1}): C, 89.24; H, 6.08. Found: C, 91.37; H, 6.97%. ^1H NMR (400 MHz, C_6D_6): δ 7.09–7.00 (m, 25H, ArH), 6.89–6.79 (m, 15H, ArH), 3.92 (br s, 4H, thf), 3.22 (s, 4H, CH_2), 1.27 (m, 4H, thf). $^{13}C\{^1H\}$ NMR (101 MHz, C_6D_6): δ 138.4 (s), 138.0 (s), 132.1 (s), 131.7 (s), 127.4 (s), 125.6 (s), 125.0 (s), 124.5 (s), 121.7 (s), 117.4 (s), 32.0 (s), 27.5 (s), 23.1 (s), 14.3 (s). IR (Nujol, cm^{-1}): 1948 m, 1879 m, 1804 m, 1752 m, 1671 w, 1596 s, 1575 w, 1310 w, 1261 m, 1176 m, 1155 m, 1096 m, 1071 s, 1027 m, 1006 m, 910 m, 858 m, 839 m, 788 m, 769 w, 747 m, 697 s.

$[Ca(C_5Ph_4CH_2)_2(thf)]$ (2). A Schlenk flask was charged with 1,2,3,4-tetraphenylfulvene (0.220 g, 0.576 mmol), freshly filed calcium metal (0.040 g, 1.00 mmol) and a crystal of iodine. Anhydrous THF (5 mL) was added, and the reaction mixture stirred for 72 hours. The resulting suspension was allowed to settle, and the supernatant solution isolated by cannula filtration. The solvent was concentrated under reduced pressure, and left to stand, affording **2** as an orange-red precipitate (0.105 g, 40%). Crystals of **2·3 THF** for determining the connectivity were obtained upon standing from a concentrated THF solution. ^1H NMR (C_6D_6, 400 MHz, 25 °C): δ 7.13–6.74 (m, 40H, ArH), 3.65 (m, 12H, thf), 3.43 (s, 4H, CH_2), 1.38 (m, 12H, thf). $^{13}C\{^1H\}$ NMR (C_6D_6, 101 MHz, 25 °C): δ 134.2 (s), 131.5 (s), 131.3 (s), 128.6 (s), 128.4 (s), 128.1 (s), 127.0 (s), 126.6 (s), 126.5 (s), 124.0 (s), 27.9 (s). MS (MALDI TOF): *m*/*z* (calc for $C_{60}H_{44}Ca$) = 805.07, *m*/*z* (found for $C_{60}H_{44}Ca$) = 805.55. IR (Nujol, cm^{-1}): 1936 w, 1794 w, 1594 m, 1574 s, 1492 w, 1329 w,

1307w, 1260 w, 1174 w, 1155 w, 1099 w, 1071 m, 1026 m, 1015 m, 902 w, 863 w, 839 w, 796 w, 787 w, 750 m, 696 m.

$[Sr(C_5Ph_4CH_2)_2(thf)_2]$ (3). The synthesis of **3** was carried out in the same way as that of **1**, but with strontium metal filings (0.100 g, 1.15 mmol) in place of magnesium metal. After 72 hours, the solid material was allowed to settle, and the supernatant solution isolated by filtration, and dried under reduced pressure and washed with *n*-hexane, affording **3** as a gold powder (0.16 g, 72%). Colourless crystals of **3·3 THF** were grown from a THF solution. Anal. calc. for $C_{72}H_{68}O_3Sr$ (1068.93 g mol^{-1} after loss of two lattice THF): C, 80.90; H, 6.41. Found: C, 80.96; H, 6.52%. ^{1}H NMR (400 MHz, C_6D_6): δ 7.09–6.99 (m, 25H, ArH), 6.89–6.76 (m, 15H, ArH), 3.60 (br s, 12H, thf), 3.49 (s, 4H, CH_2), 1.36 (br s, 12H, thf). $^{13}C\{^1H\}$ NMR (101 MHz, C_6D_6): δ 139.7 (s), 138.9 (s), 132.0 (s), 130.5 (s), 128.7 (s), 127.3 (s), 126.2 (s), 125.5 (s), 124.8 (s), 124.6 (s), 68.9 (s, thf) 27.6 (s), 25.5 (s, thf). IR (Nujol, cm^{-1}): 1941 w, 1876 w, 1806 w, 1593 s, 1574 m, 1259 w, 1177 m, 1154 m, 1122 w, 1099 w, 1071 m, 1026 s, 907 m, 870 m, 789 m, 770 m, 743 s, 696 s, 616 w, 557 w.

$[Ba(C_5Ph_4CH_2)_2(thf)_2]$ (4). The synthesis of **4** was carried out in the same way as that of **1**, but with barium metal filings (0.137 g, 1.00 mmol) in place of magnesium metal. After filtration the solution was concentrated to ~2 mL and allowed to stand at room temperature, yielding large colourless crystals of **4·2 THF** (0.105 g, 38%). Anal. calc. for $C_{68}H_{60}O_2Ba$ (1046.53 g mol^{-1} after loss of 2 lattice THF): C, 78.04; H, 5.78. Found: C, 78.88; H, 6.10%. ^{1}H NMR (400 MHz, C_6D_6): δ 7.08–6.99 (m, 26H, ArH), 6.83 (tt, 9H, ArH), 6.76 (tt, 5H, ArH), 3.48 (br s, 16H, thf), 3.43 (s, 4H, CH_2), 1.35 (br s, 16H, thf) on single crystals. $^{13}C\{^1H\}$ NMR (101 MHz, C_6D_6): δ 139.9 (s), 139.5 (s), 131.8 (s), 130.8 (s), 128.6 (s), 127.3 (s), 127.3 (s), 125.8 (s), 124.8 (s), 124.3 (s), 68.0 (s), 27.2 (s), 25.5 (s). IR (Nujol, cm^{-1}): 1958 m, 1883 m, 1805 m, 1743 m, 1596 s, 1575 w, 1328 w, 1308 w, 1257 w, 1180 m, 1155 w, 1125 w, 1068 m, 1028 m, 909 m, 790 m, 771 w, 744 m, 695 m.

$[Fe(C_5Ph_4CH_2)_2]$ (5). A vial was charged with **2** (0.100 g, 0.124 mmol), $FeCl_2$ (0.016 g, 0.126 mmol), and anhydrous THF (1 mL). The reaction mixture was stirred for 24 hours before filtering and concentrating, affording **5** as a red powder (0.096 g, 94%). Single crystals suitable for XRD studies of **5·2 THF** were obtained from a saturated THF/pentane solution at −20 °C. ^{1}H NMR (THF-d_8, 400 MHz, 25 °C): δ 7.50–7.24 (m, 8H, ArH), 7.22–7.06 (m, 8H, ArH), 7.05–6.86 (m, 16H, ArH), 6.83–6.61 (m, 8H, ArH), 3.25 (s, 4H, CH_2). $^{13}C\{^1H\}$ NMR (THF-d_8, 100 MHz, 25 °C): δ 137.1, 134.4, 134.1, 133.2, 131.5, 127.7, 127.6, 127.2, 126.7, 95.0, 94.0, 82.7, 33.6. UV/vis: nm ($CDCl_3$) 500, 340, 303, 272. HRMS (ESI$^+$): m/z $[M + H]^+$ calc. for $C_{60}H_{45}Fe$: 821.2871; found: 821.2852. IR (ATR) ν/cm^{-1}: 3381, 3053, 1948, 1599, 1499, 1443, 1260, 1155, 1094, 1069, 1026, 913, 799, 749, 693, 654, 618, 585.

Crystal and refinement data

Single crystals covered with viscous hydrocarbon oil were mounted on a Kapton loop. Data for complex **1·Toluene** and **5·2 THF** were obtained at −123 °C (150 K) on a Stoe Stadivari diffractometer equipped with an EIGER2 1M CdTe detector and a Mo microfocus source. Data for complex **3·3 THF** were obtained on the MX1: Macromolecular Crystallography beamline at the Australian Synchrotron, Victoria, Australia. Data for complexes **2·3 THF** and **4·2 THF** were obtained at −150 °C (123 K) and were measured on a Rigaku SynergyS diffractometer. The SynergyS operated using microsource Mo-Kα radiation (λ = 0.71073 Å) and Cu-Kα radiation (λ = 1.54184 Å). Data collection and integration on the MX1: macromolecular crystallography beamline was accomplished using Blu-Ice.[79] For complex **4·2 THF**, data processing was conducted using CrysAlisPro.55 software suite.[80] Solid-state structures were solved using the SHELXS-97 or SHELXT programs in conjunction with the X-Seed graphical user interface.[81–83] The refinement was performed with the SHELXL program[84] using Olex2.[85] All hydrogen atoms were placed in calculated positions utilising the riding model.

Conclusions

A series of *ansa*-bridged alkaline earth octaphenylmetallocene complexes from Mg to Ba was synthesised *via* reductive dimerisation of 1,2,3,4-tetraphenylfulvene. The complexes were fully characterised by multinuclear NMR spectroscopy and SC-XRD. In the case of Sr, **3** represents the first structurally characterised *ansa*-metallocene, whereas for the Ba complex **4**, the stability of this *ansa* complex is significantly increased with respect to the non-bridged analogue. The solid-state structures revealed a notable ring-slippage for the Mg complex towards η^3 like bonding, and to a lesser extent, for the Ba complex. For the latter, the ethylene bridge was less twisted compared to the other complexes with smaller cations. The Ca-*ansa* complex was successfully employed in the transmetallation of the ligand onto Fe(II) providing a new air-stable bent Fe-*ansa* complex **5** with solution properties similar to those of the linear non-bridged octaphenylferrocene. Studies concerning the full synthetic potential and the reactivity, especially in small molecule activation, of the new group 2 metal *ansa* complexes is underway,[39,40,86] as well as investigations into the synthesis of metallopolymers based on the new *ansa*-ferrocene.[72,73]

Author contributions

ACGS, AB and AD performed the experimental work. ZG, SC and TS performed XRD measurements and solved the crystal structures. CN and OD undertook the electrochemistry experiments. ACGS and FJ prepared the manuscript with the help of GBD and PCJ. All authors contributed to the preparation of the SI. GBD, PCJ and FJ oversaw the project.

Conflicts of interest

There are no conflicts to declare.

Data availability

The data supporting this article have been included as part of the SI (^{1}H NMR, ^{13}C NMR and IR spectra of all new complexes, UV/vis spectrum and electrochemical data on complex **5**, additional information on X-ray crystallography, determination of slip parameter). See DOI: **https://doi.org/10.1039/d5dt01881a**.

CCDC 2464826 for **1**, 2464827–2464829 for **3–5** contain the supplementary crystallographic data for this paper.[88a–d]

Acknowledgements

ACGS would like to acknowledge the Australian Government's support of this research through an Australian Government Research Training Program scholarship. AD thanks the Région Grand Est (France) and the JCU for a PhD scholarship (project EURO2LUM). The CNRS, the University of Reims Champagne-Ardenne, the Ecole Nationale Supérieure de Chimie de Montpellier (ENSCM), the Université de Montpellier are acknowledged for financial support. The authors also thank the Balard Platform for Analysis and Characterisation (PAC Balard) facilities for technical support. The authors acknowledge support by the Australian Research Council (DP230100112). Part of this work was conducted using the MX1 beamline at the Australian Synchrotron, which is part of ANSTO,[87] and the DIFFRAX platform (X-Ray diffraction at Ecole Polytechnique, IPParis).

References

1 P. J. Shapiro, *Coord. Chem. Rev.*, 2002, **231**, 67–81.
2 D. E. Herbert, U. F. J. Mayer and I. Manners, *Angew. Chem., Int. Ed.*, 2007, **46**, 5060–5081.
3 C. E. Zachmanoglou, A. Docrat, B. M. Bridgewater, G. Parkin, C. G. Brandow, J. E. Bercaw, C. N. Jardine, M. Lyall, J. C. Green and J. B. Keister, *J. Am. Chem. Soc.*, 2002, **124**, 9525–9546.
4 H. Braunschweig and F. M. Breitling, *Coord. Chem. Rev.*, 2006, **250**, 2691–2720.
5 B. Wang, *Coord. Chem. Rev.*, 2006, **250**, 242–258.
6 A. S. Rodrigues, E. Kirillov and J. F. Carpentier, *Coord. Chem. Rev.*, 2008, **252**, 2115–2136.
7 D. B. Culver, J. Corieri, G. Lief and M. P. Conley, *Organometallics*, 2022, **41**, 892–899.
8 M. B. Laing and K. N. Trueblood, *Acta Crystallogr.*, 1965, **19**, 373–381.
9 H. Schnutenhaus and H. H. Brintzinger, *Angew. Chem., Int. Ed.*, 1979, **18**, 777–778.
10 W. Kaminsky, K. Külper, H. H. Brintzinger and F. R. W. P. Wild, *Angew. Chem., Int. Ed.*, 1985, **24**, 507–508.
11 M. A. Bau, S. Wiesler, S. L. Younas and J. Streuff, *Chem. – Eur. J.*, 2019, **25**, 10531–10545.
12 L. Stieglitz, D. Henschel, T. Pehl and B. Rieger, *Organometallics*, 2021, **40**, 4055–4065.
13 P. S. Kulyabin, G. P. Goryunov, M. I. Sharikov, V. V. Izmer, A. Vittoria, P. H. M. Budzelaar, V. Busico, A. Z. Voskoboynikov, C. Ehm, R. Cipullo and D. V. Uborsky, *J. Am. Chem. Soc.*, 2021, **143**, 7641–7647.
14 X. Desert, F. Proutiere, A. Welle, K. D. Dauw, A. Vantomme, O. Miserque, J. M. Brusson, J. F. Carpentier and E. Kirillov, *Organometallics*, 2019, **38**, 2664–2673.
15 P. V. Kovyazin, L. M. Khalilov and L. V. Parfenova, *Molecules*, 2025, **30**, 2511.
16 I. A. Bischoff, R. S. Meme, M. S. Bhatti, B. Morgenstern and A. Schäfer, *Organometallics*, 2022, **41**, 3781–3787.
17 H. Bhattacharjee, S. Dey, J. Zhu, W. Sun and J. Müller, *Chem. Commun.*, 2018, **54**, 5562–5565.
18 P. J. Shapiro, P. J. Sinnema, P. Perrotin, P. H. M. Budzelaar, H. Weihe, B. Twamley, R. A. Zehnder and J. J. Nairn, *Chem. – Eur. J.*, 2007, **13**, 6212–6222.
19 S. Mondal, S. Sarkar, C. Mandal, D. Mallick and D. Mukherjee, *Chem. Commun.*, 2024, **60**, 4553–4556.
20 S. Usuba, S. Morisako, K. Masada, K. Sugamata and T. Sasamori, *Molecules*, 2025, **30**(6), 1361.
21 S. L. J. Conway, L. H. Doerrer, M. L. H. Green and M. A. Leech, *Organometallics*, 2000, **19**, 630–637.
22 S. Weller, R. Klenk, Z. Kelemen, L. Nyulászi, M. Nieger and D. Gudat, *Eur. J. Inorg. Chem.*, 2022, **2022**, e202100923.
23 P. Sinnema, P. J. Shapiro, D. Min, J. Foo and B. Twamley, *J. Am. Chem. Soc.*, 2002, **2002**, 10996–10997.
24 J. C. Wedal, L. M. Anderson-Sanchez, M. T. Dumas, C. A. Gould, M. J. Beltrán-Leiva, C. Celis-Barros, D. Páez-Hernández, J. W. Ziller, J. R. Long and W. J. Evans, *J. Am. Chem. Soc.*, 2023, **145**, 10730–10742.
25 C. Wang, L. Xiang, X. Leng and Y. Chen, *Organometallics*, 2016, **35**, 1995–2002.
26 E. Laur, E. Louyriac, V. Dorcet, A. Welle, A. Vantomme, O. Miserque, J. M. Brusson, L. Maron, J. F. Carpentier and E. Kirillov, *Macromolecules*, 2017, **50**, 6539–6551.
27 P. Preethalayam, K. S. Krishnan, S. Thulasi, S. S. Chand, J. Joseph, V. Nair, F. Jaroschik and K. V. Radhakrishnan, *Chem. Rev.*, 2017, **117**, 3930–3989.
28 J. J. Eisch, F. A. Owuor and X. Shi, *Polyhedron*, 2005, **24**, 1325–1339.
29 A. Recknagel and F. T. Edelmann, *Angew. Chem., Int. Ed.*, 1991, **30**, 693–694.
30 M. Rieckhoff, U. Pieper, D. Stalke and F. T. Edelmann, *Angew. Chem., Int. Ed.*, 1993, **32**, 1079–1081.
31 P. J. Sinnema, P. J. Shapiro, B. Höhn, T. E. Bitterwolf and B. Twamley, *Organometallics*, 2001, **20**, 2883–2888.
32 A. Recknagel, F. T. Edelmann, M. Rieckhoff, I. Haiduc, U. Pieper, D. Stalke, K. M. Kane, P. J. Shapiro, R. Cubbon, A. Vij, A. L. Rheingold, P.-J. Sinnema, B. Höhn, T. E. Bitterwolf and B. Twamley, *Organometallics*, 2001, **21**, 182–191.
33 P. Dabringhaus, M. Schorpp, H. Scherer and I. Krossing, *Angew. Chem., Int. Ed.*, 2020, **59**, 22023–22027.
34 N. Leyser, K. Schmidt and H. H. Brintzinger, *Organometallics*, 1998, **17**, 2155–2161.
35 S. Baguli, S. Mondal, C. Mandal and S. Goswami, *Chem. – Asian J.*, 2022, **17**, e202100962.

36 L. Wirtz and A. Schäfer, *Chem. – Eur. J.*, 2021, **27**, 1219–1230.
37 K. Strohfeldt and M. Tacke, *Chem. Soc. Rev.*, 2008, **37**, 1174–1187.
38 M. Kessler, S. Hansen, C. Godemann, A. Spannenberg and T. Beweries, *Chem. – Eur. J.*, 2013, **19**, 6350–6357.
39 L. Wirtz, J. Lambert, B. Morgenstern and A. Schäfer, *Organometallics*, 2021, **40**, 2108–2117.
40 L. Wirtz, W. Haider, V. Huch, M. Zimmer and A. Schäfer, *Chem. – Eur. J.*, 2020, **26**, 6176–6184.
41 W. P. Oziminski, *J. Organomet. Chem.*, 2012, **708–709**, 10–17.
42 J. J. Antonio and E. Kraka, *Phys. Chem. Chem. Phys.*, 2024, **26**, 15143–15155.
43 T. P. Hanusa, *Organometallics*, 2002, **21**, 2559–2571.
44 P. S. Tanner and T. P. Hanusa, *Polyhedron*, 1994, **13**, 2417–2420.
45 L. Orzechowski, D. F. J. Piesik, C. Ruspic and S. Harder, *Dalton Trans.*, 2008, **35**, 4742–4746.
46 G. B. Deacon, F. Jaroschik, P. C. Junk and R. P. Kelly, *Organometallics*, 2015, **34**, 2369–2377.
47 X. Shi, G. Qin, Y. Wang, L. Zhao, Z. Liu and J. Cheng, *Angew. Chem., Int. Ed.*, 2019, **58**, 4356–4360.
48 G. B. Deacon, C. M. Forsyth, F. Jaroschik, P. C. Junk, D. L. Kay, T. Maschmeyer, A. F. Masters, J. Wang and L. D. Field, *Organometallics*, 2008, **27**, 4772–4778.
49 Y. Schulte, H. Weinert, C. Wölper and S. Schulz, *Organometallics*, 2020, **39**, 206–216.
50 A. C. G. Shephard, A. Delon, S. Chevreux, A. Martinez, Z. Guo, G. B. Deacon, G. Lemercier, N. McClenaghan, G. Jonusauskas, P. C. Junk and F. Jaroschik, *Inorg. Chem.*, 2024, **63**, 9395–9405.
51 H. Jacobsen and P. Burger, *Chimia*, 1996, **50**, 329.
52 J. W. Faller, R. H. Crabtree and A. Habib, *Organometallics*, 1985, **4**, 929–935.
53 I. Honzíčková, J. Vinklárek, C. C. Romão, Z. Růžičková and J. Honzíček, *New J. Chem.*, 2016, **40**, 245–256.
54 F. M. Chadwick, A. E. Ashley, R. T. Cooper, L. A. Bennett, J. C. Green and D. M. O'Hare, *Dalton Trans.*, 2015, **44**, 20147–20153.
55 A. Jaenschke, F. Olbrich and U. Behrens, *Z. Anorg. Allg. Chem.*, 2009, **635**, 2550–2557.
56 H. J. Sanderson, G. Kociok-Kohn and U. Hintermair, *Inorg. Chem.*, 2023, **62**, 15983–15991.
57 H. R. H. Damrau, A. Geyer, M. H. Prosenc, A. Weeber, F. Schaper and H. H. Brintzinger, *J. Organomet. Chem.*, 1998, **553**, 331–343.
58 G. J. Matare, K. M. Kane, P. J. Shapiro and A. Vij, *J. Chem. Crystallogr.*, 1998, **28**, 731–734.
59 R. D. Shannon, *Acta Crystallogr., Sect. A: Found. Crystallogr.*, 1976, **32**, 751–767.
60 M. J. Harvey, K. T. Quisenberry, T. P. Hanusa and V. G. Young, *Eur. J. Inorg. Chem.*, 2003, **2003**, 3383–3390.
61 R. A. Williams, K. F. Tesh and T. P. Hanusa, *J. Am. Chem. Soc.*, 1991, **113**, 4843–4851.
62 M. P. Castellani, J. M. Wright, S. J. Geib, A. L. Rheingold and W. C. Trogler, *Organometallics*, 1986, **5**, 1116–1122.
63 K.–H. Thiele, F. Rehbaum, H. Baumann, H. Schumann, F. H. Görlitz and R. Weimann, *Z. Anorg. Allg. Chem.*, 1992, **613**, 76–82.
64 M. P. Castellani, S. J. Geib, A. L. Rheingold and W. C. Trogler, *Organometallics*, 1987, **6**, 1703–1712.
65 J. E. Collins, M. P. Castellani, A. L. Rheingold, E. J. Miller, W. E. Geiger, A. L. Rieger, P. H. Rieger, D. Chemistry and W. Virginia, *Organometallics*, 1995, **14**, 1232–1238.
66 R. J. Hoobler, J. V. Adams, M. A. Hutton, T. W. Francisco, B. S. Haggerty, A. L. Rheingold and M. P. Castellani, *J. Organomet. Chem.*, 1991, **412**, 157–167.
67 S. Barlow, M. J. Drewitt, T. Dijkstra, J. C. Green, D. O'Hare, C. Whittingham, H. H. Wynn, D. P. Gates, I. Manners, J. M. Nelson and J. K. Pudelski, *Organometallics*, 1998, **17**, 2113–2120.
68 M. Tanabe, S. C. Bourke, D. E. Herbert, A. J. Lough and I. Manners, *Angew. Chem., Int. Ed.*, 2005, **44**, 5886–5890.
69 A. Nezamzadeh, J. Zhu and J. Müller, *Organometallics*, 2024, **43**, 1119–1127.
70 V. S. Ajithkumar, M. K. Bisai, K. Yuvaraj, R. G. Gonnade and S. S. Sen, *Eur. J. Inorg. Chem.*, 2025, **28**, e202500120.
71 S. A. Bezawada, N. Ušto, C. Wilke, M. Barnes-Flaspoler, R. Jagan and E. B. Bauer, *Molecules*, 2023, **28**, 2729.
72 J. B. Gilroy, A. D. Russell, A. J. Stonor, L. Chabanne, S. Baljak, M. F. Haddow and I. Manners, *Chem. Sci.*, 2012, **3**, 830–841.
73 D. E. Herbert, U. F. J. Mayer, J. B. Gilrov, M. J. López-Gómez, A. J. Lough, J. P. H. Charmant and I. Manners, *Chem. – Eur. J.*, 2009, **15**, 12234–12246.
74 M. Cybulski, O. Michalak, W. Buchowicz and M. Mazur, *Molecules*, 2024, **29**, 4903.
75 H. Schumann, A. Lentz, R. Weimann and J. Pickardt, *Angew. Chem., Int. Ed.*, 1994, **33**, 1731–1733.
76 J. M. Nelson, P. Nguyen, R. Petersen, H. Rengel, P. M. Macdonald, A. J. Lough, I. Manners, N. P. Raju, J. E. Greedan, S. Barlow and D. O'Hare, *Chem. – Eur. J.*, 1997, **3**, 573–584.
77 H. L. Lentzner and W. E. Watts, *J. Chem. Soc. D: Chem. Commun.*, 1970, 26–27.
78 H. L. Lentzner and W. E. Watts, *Tetrahedron*, 1971, **27**, 4343–4351.
79 T. M. McPhillips, S. E. McPhillips, H. J. Chiu, A. E. Cohen, A. M. Deacon, P. J. Ellis, E. Garman, A. Gonzalez, N. K. Sauter, R. P. Phizackerley, S. M. Soltis and P. Kuhn, *J. Synchrotron Radiat.*, 2002, **9**, 401–406.
80 *CrysAlisPRO v.39. Yarnton*, Agilent Technologies Ltd, Oxfordshire, England.
81 G. M. Sheldrick, *Acta Crystallogr.*, 2008, **64**, 112–122.
82 G. M. Sheldrick, *Acta Crystallogr.*, 2015, **71**, 3–8.
83 L. J. Barbour, *J. Supramol. Chem.*, 2001, **1**, 189–191.
84 G. M. Sheldrick, *Acta Crystallogr., Sect. C: Struct. Chem.*, 2015, **71**, 3–8.
85 O. V. Dolomanov, L. J. Bourhis, R. J. Gildea, J. A. K. Howard and H. Puschmann, *J. Appl. Crystallogr.*, 2009, **42**, 339–341.

86 B. Rösch and S. Harder, *Chem. Commun.*, 2021, **57**, 9354–9365.
87 N. P. Cowieson, D. Aragao, M. Clift, D. J. Ericsson, C. Gee, S. J. Harrop, N. Mudie, S. Panjikar, J. R. Price, A. Riboldi-Tunnicliffe, R. Williamson and T. Caradoc-Davies, *J. Synchrotron Radiat.*, 2015, **22**, 187–190.
88 (*a*) A. C. G. Shephard, A. Bouammali, A. Delon, Z. Guo, S. Chevreux, C. Niebel, O. Dautel, T. Simler, G. B. Deacon, P. C. Junk and F. Jaroschik, CCDC 2464826: Experimental Crystal Structure Determination, 2025, DOI: **10.5517/ccdc.csd.cc2nqvjs**; (*b*) A. C. G. Shephard, A. Bouammali, A. Delon, Z. Guo, S. Chevreux, C. Niebel, O. Dautel, T. Simler, G. B. Deacon, P. C. Junk and F. Jaroschik, CCDC 2464827: Experimental Crystal Structure Determination, 2025, DOI: **10.5517/ccdc.csd.cc2nqvkt**; (*c*) A. C. G. Shephard, A. Bouammali, A. Delon, Z. Guo, S. Chevreux, C. Niebel, O. Dautel, T. Simler, G. B. Deacon, P. C. Junk and F. Jaroschik, CCDC 2464828: Experimental Crystal Structure Determination, 2025, DOI: **10.5517/ccdc.csd.cc2nqvlv**; (*d*) A. C. G. Shephard, A. Bouammali, A. Delon, Z. Guo, S. Chevreux, C. Niebel, O. Dautel, T. Simler, G. B. Deacon, P. C. Junk and F. Jaroschik, CCDC 2464829: Experimental Crystal Structure Determination, 2025, DOI: **10.5517/ccdc.csd.cc2nqvmw**.